

## Crystal Growth of Electronic Ferroelectric, $\text{YbFe}_2\text{O}_4$ Film

\*Tomoko Nagata<sup>1</sup>, Nobuyuki Iwata<sup>1</sup> and Hiroshi Yamamoto<sup>1</sup>

**Abstract:** In order to realize the ultra fast switching of the electric polarization, crystal growth of electronic ferroelectric,  $\text{YbFe}_2\text{O}_4$  film was investigated. The film was deposited on *c*-oriented  $\text{Al}_2\text{O}_3$  substrate using pulsed laser deposition method. Well oriented film was fabricated although the mixture phase of hexagonal (h-)  $\text{YbFeO}_3$ ,  $\text{Yb}_2\text{O}_3$ ,  $\text{Fe}_3\text{O}_4$  was obtained. Pole figures indicated the growth of well-crystalline h- $\text{YbFeO}_3$ , which has quite similar crystal structure to that of  $\text{YbFe}_2\text{O}_4$ . Crystal structure of improved film will be discussed.

### 1. Introduction

Much effort has been made to design functional materials with multi-ferroicity. If the ferroelectricity arises from the configuration of *3d* electrons having different valence states, the direct coupling is expected between the ferroelectricity and magnetic property. Moreover, the electronic origin has advantages in the energy and the speed for the switching, comparing to the ordinal ferroelectrics.

$\text{RFe}_2\text{O}_4$  (*R* = rare earth ions) had been proposed as a candidate of such materials [1].  $\text{RFe}_2\text{O}_4$  is composed of doubly stacking iron triangular layers (*W*-layer) separated by single rare-earth triangular layer (*R*-layer) (Fig. 1). The equal amounts of  $\text{Fe}^{2+}$  and  $\text{Fe}^{3+}$  exist on the triangular lattices and the charge- and magnetic-orderings take place. The magnetic ordering is known to exhibit ferri-magnetism and the charge ordering is proposed to generate ferroelectricity [1]. If each *W*-layer consists of  $\text{Fe}^{2+}$  rich Fe-layer and  $\text{Fe}^{3+}$  rich Fe-layer, each *W*-layer has microscopic electric polarization and their in-phase stacking generates ferroelectricity. As this ferroelectricity arises from electronic configuration, it has been called “electronic ferroelectricity” [2].

Although the existense of the electronic ferroelectricity had been questioned for recent decades [3], we succeeded in proving it by electric measurements and x-ray diffraction experiments [4,5]. We showed a clear polarization hysteresis loop as a function of applied electric field (*P-E* loop) in  $\text{YbFe}_2\text{O}_4$ . The ferroelectric transition temperatures were determined as 300 K and 100 K from the pyroelectric current measurements. As these temperatures are in good agreement with the developing teperature of the charge ordering, we concluded that the charge ordering is responsible for the ferroelectricity.

However, we found that the ferroelectric charge ordering coexist with antiferroelectric charge ordering, which is a little more stable. Therefore the majority phase was observed as the antiferroelectric in bulk. Although we also found that the electric field cooling enhances the formation

of the ferroelectric phase [4,5], simple method to get single ferroelectric phase is required for the application.

One of the routes is to fabricate the thin film because thin film has the advantage in controlling the lattice parameter. The change of the lattice parameter may generate the difference in the electric interaction between iron ions. In this study, we investigated the crystal growth of  $\text{YbFe}_2\text{O}_4$  film using pulsed laser deposition (PLD) method.

### 2. Experimental detail

A thin film was deposited on  $\text{Al}_2\text{O}_3(0001)$  at  $730^\circ\text{C}$  by PLD method using KrF excimer laser (energy density =  $2.5 \text{ J/cm}^2$ , repetition rate = 1 Hz). During the deposition process, oxygen gas was flowed and the pressure was  $7.2 \times 10^{-5} \text{ Pa}$ . The surface molohology was observed by atomic force microscope (AFM) (SII). The crystal structure was investigated from x-ray diffraction experiments ( $2\theta$ - $\theta$  scan and pole figure) and depth profile of the atmic concentration using x-ray photoelectron spectroscopy with ion beam etching (ESCA-3400).

### 3. Results and Discussion

Fig. 2 shows the AFM images of the film surface. The surface consisted of  $1 \mu\text{m}$  size of triangle shape grains. The step-terrace structure was observed in each grain although the height of the step was as high as  $\sim 5 \text{ nm}$ .

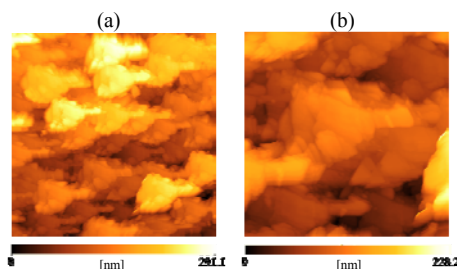


Fig. 2 AFM images of the film surface. (a)  $5 \times 5 \mu\text{m}$ , (b)  $2 \times 2 \mu\text{m}$ .

Fig. 3 shows the  $2\theta$ - $\theta$  x-ray diffraction pattern of the film. Three kinds of phase were obtained; hexagonal (h-)  $\text{YbFeO}_3$ ,  $\text{Yb}_2\text{O}_3$  and  $\text{Fe}_3\text{O}_4$ . h- $\text{YbFeO}_3$  consists of alternating stacking of Fe-layer and Yb-layer, which is quite similar crystal structure to that of  $\text{YbFe}_2\text{O}_4$ . Although  $\text{YbFe}_2\text{O}_4$  phase was not obtained, all phases were well oriented, which is consistent with the layered structure on the surface (Fig. 2).

<sup>1</sup> : Department of Electronic Engineering, College of Science and Technology, Nihon University.

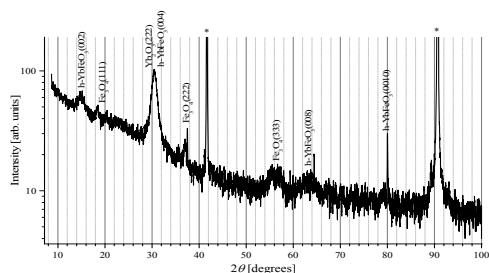


Fig. 3  $2\theta$ - $\theta$  x-ray diffraction pattern of the film. The asterisk indicates the peak arising from the  $\text{Al}_2\text{O}_3$  substrate.

In order to understand the in-plane orientation of the film, pole figures were obtained. Fig. 4 shows the pole figures around (a)  $2\theta = 30^\circ, 40^\circ$ , (b)  $15^\circ$ , (c)  $35^\circ$  and  $65^\circ$ . Comparing  $2\theta$  values of powder diffraction patterns [6-8], the origin of the observed peaks can be estimated as follows;  $\text{Al}_2\text{O}_3$  for  $2\theta = 40^\circ$ , h-YbFeO<sub>3</sub> for  $2\theta = 15^\circ$ , Yb<sub>2</sub>O<sub>3</sub> for  $2\theta = 30^\circ$ , and Fe<sub>3</sub>O<sub>4</sub> for  $2\theta = 35^\circ$  and  $65^\circ$ .

As shown in Fig. 4(a),  $\text{Al}_2\text{O}_3$  substrate showed two peaks having  $120^\circ$  angle between each other, which is consistent with the three-fold axis. Around  $2\theta = 15^\circ$ , h-YbFeO<sub>3</sub> showed only one peak in the angle area showed in Fig. 4(b), indicating the existence of the three fold axis. As the  $\phi$  position is the same as that of  $\text{Al}_2\text{O}_3$ , it is indicated that h-YbFeO<sub>3</sub> had the same orientation as that of  $\text{Al}_2\text{O}_3$ . The existence of the clear three-fold axis suggests the well-crystalline h-YbFeO<sub>3</sub> film. Around  $2\theta = 30^\circ$ , Yb<sub>2</sub>O<sub>3</sub> showed doubly splitting peaks around  $30^\circ$  tilting point to  $\text{Al}_2\text{O}_3$  in-plane, indicating that the Yb<sub>2</sub>O<sub>3</sub> grew with lower symmetry and in-plane tilting angle of  $30^\circ$  to  $\text{Al}_2\text{O}_3$  (Fig. 4(a)). Around  $2\theta = 35^\circ$  and  $65^\circ$ , Fe<sub>3</sub>O<sub>4</sub> showed two sets of six peaks, indicating the existence of two kinds of grains having in-plane tilting angle of  $30^\circ$  to each other (Fig. 4(c)). The intensity of one set of peaks was a little lower at the same  $\phi$  position as that of  $\text{Al}_2\text{O}_3$ , indicating that the majority Fe<sub>3</sub>O<sub>4</sub> grains have  $30^\circ$  of in-plane tilting angle to  $\text{Al}_2\text{O}_3$ . The six fold axes may indicate some stacking faults of Fe<sub>3</sub>O<sub>4</sub>. The two sets of peaks suggest that Fe<sub>3</sub>O<sub>4</sub> phase appeared twice during the growing process due to the change of the growing condition or lattice matching with neighboring layers having different phases.

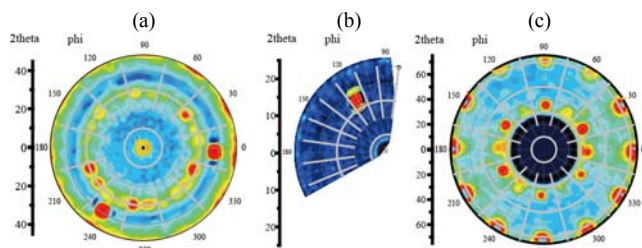


Fig. 4 pole figures around (a)  $2\theta = 30^\circ, 40^\circ$ , (b)  $15^\circ$ , (c)  $35^\circ$  and  $65^\circ$ .

In order to investigate the relation between the growing phase and growing condition or lattice matching, depth profile of the atomic concentration was obtained. Fig. 5 shows the etching time dependence of the atomic

concentration ratio of Fe/Yb. The Fe:Yb ratio was 1:1 at the initial stage of the growth. With increasing the growing time, the Fe:Yb ratio increased to 2 and decrease to 1. At the final stage, the Fe:Yb ratio increased toward 2 again. This result suggests the formation of h-YbFeO<sub>3</sub> at the initial stage followed by the successive growths of Fe<sub>3</sub>O<sub>4</sub> and Yb<sub>2</sub>O<sub>3</sub>. At the final stage Fe<sub>3</sub>O<sub>4</sub> may have grown again.

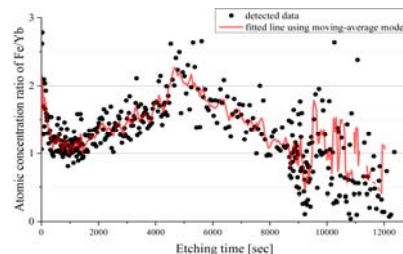


Fig. 5 Depth profile of the atomic concentration ratio of Fe/Yb. The data was fitted using moving-average model.

As for the average Fe/Yb ratio, it was smaller than 2 in total. This result suggests that Fe atom vaporization during deposition due to its lower vapor pressure than Yb. The quite low back pressure during the deposition may have enhanced the vaporization of Fe atom by keeping the collision speed high to the substrate. The inactive gas is required to increase the back pressure and decrease the collision speed. Another way to get YbFe<sub>2</sub>O<sub>4</sub> phase may be to decrease the oxygen partial pressure. The pole figures indicated that the two kinds of iron oxides showed quite different crystalline; h-YbFeO<sub>3</sub> showed much more good crystalline than Fe<sub>3</sub>O<sub>4</sub>. Although the crystal structure is of course included as one of the origins of this difference, the valence of Fe ions may also responsible for the difference. The average valence of Fe ion in Fe<sub>3</sub>O<sub>4</sub> is  $+8/3$ , which is lower than  $+3$  in h-YbFeO<sub>3</sub>. As that of YbFe<sub>2</sub>O<sub>4</sub> is  $+5/2$  and lower than Fe<sub>3</sub>O<sub>4</sub>, its stable oxygen partial pressure may be lower.

#### 4. Summary

The crystal growth of YbFe<sub>2</sub>O<sub>4</sub> film was investigated using PLD method. Well-oriented mixture phase of h-YbFeO<sub>3</sub>, Yb<sub>2</sub>O<sub>3</sub> and Fe<sub>3</sub>O<sub>4</sub> was obtained. The crystal structure of improved film will be discussed.

#### 5. References

- [1] N. Ikeda *et al.*, Nature **436** (2005) 1136.
- [2] T. Portengen *et al.*, Phys. Rev. B **54** (1996) 17452.
- [3] M. Angst, Phys. Status Solidi: Rapid Res. Lett. **7** (2013) 383.
- [4] T. Nagata, PhD thesis, Okayama University (2014).
- [5] T. Nagata *et al.*, in progress.
- [6] L.J. Downie *et al.*, J. Solid State Chemi. **190** (2012) 52.
- [7] B.A. Wechsler *et al.*, American Mineralogist **69** (1984) 754.
- [8] C. Haavik American Mineralogist **85** (2000) 514.